SPE: Polymer Engineering & Science Published by John Wiley & Sons, Inc.

Dear Author,

Your article page proofs for SPE: Polymer Engineering & Science are ready for your final content correction within our rapid production workflow. The PDF file found at the URL given below is generated to provide you with a proof of the content of your manuscript. Once you have submitted your corrections, the production office will proceed with the publication of your article.

John Wiley & Sons has made this article available to you online for faster, more efficient editing. Please follow the instructions below and you will be able to access a PDF version of your article as well as relevant accompanying paperwork.

You will need to have a copy of Adobe Acrobat Reader software to read these files. This is free software and is available for user downloading at http://www.adobe.com/products/acrobat/readstep.html.

Open your web browser, and enter the following web address:
http://115.111.50.156/jw/retrieval.aspx?pwd=01f04c008ff6

You will be prompted to log in, and asked for a password. Your login name will be your email address, and your password will be 01f04c008ff6

Example:
Login: your e-mail address
Password: 01f04c008ff6

The site contains one file, containing:

- Author Instructions Checklist
- Annotated PDF Instructions
- Reprint Order Information
- Color Reproduction Charge Form
- A copy of your page proofs for your article

In order to speed the proofing process, we strongly encourage authors to correct proofs by annotating PDF files. Any corrections should be returned to jrnlprodpen@cadmus.com 1 to 2 business days after receipt of this email in order to achieve our goal of publishing your article online 15 days from the day final data was received. Thank you for your cooperation.

Please take care to:

- answer all queries located on the last page of the PDF proof

- proofread any tables and equations carefully

- check your figure(s) and legends for accuracy

- check that any special or Greek characters (especially "mu") have converted correctly

Production Editor, PEN

E-mail: jrnlprodpen@cadmus.com

Technical problems? If you experience technical problems downloading your file or any other problem with the website listed above, please contact Balaji/Sam (e-mail: Wiley.CS@cenveo.com, phone: +91 (44) 4205-8810 (ext.308)). Be sure to include your article number.

Questions regarding your article? Trouble interpreting any of the questions listed at the end of your file? REMEMBER TO INCLUDE YOUR ARTICLE NO. (PES-13-1477.R2) WITH ALL CORRESPONDENCE. This will enable us to address your query more efficiently.
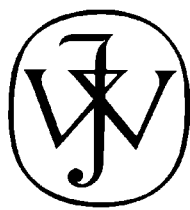
As this e-proofing system was designed to make the publishing process easier for everyone, we welcome any and all feedback. Thanks for participating in our e-proofing system!

This e-proof is to be used only for the purpose of returning corrections to the publisher.

Sincerely,

Production Editor, PEN

E-mail: jrnlprodpen@cadmus.com

WILEY
Publishers Since 1807

***POLYMER ENGINEERING AND SCIENCE* PRODUCTION**

IMMEDIATE RESPONSE REQUIRED
Your article will be published online via Wiley's EarlyView® service (wileyonlinelibrary.com) shortly after receipt of corrections. EarlyView® is Wiley's online publication of individual articles in full text HTML and/or pdf format before release of the compiled print issue of the journal. Articles posted online in EarlyView® are peer-reviewed, copyedited, author corrected, and fully citable via the article DOI (for further information, visit www.doi.org). EarlyView® means you benefit from the best of two worlds—fast online availability as well as traditional, issue based archiving.

☐ **READ PROOFS CAREFULLY**
- This will be your <u>only</u> chance to review these proofs. **Please note that once your corrected article is posted online, it is considered legally published, and cannot be removed from the Web site for further corrections.**
- Please note that the volume and page numbers shown on the proofs are for position only.

☐ **ANSWER ALL QUERIES ON PROOFS (Queries for you to answer are attached as the last page of your proof.)**
- In order to speed the proofing process, we strongly encourage authors to correct proofs by annotating PDF files. Please see the instructions on the Annotation of PDF files. If unable to annotate the PDF file, please print out and mark changes directly on the page proofs.

☐ **CHECK FIGURES AND TABLES CAREFULLY**
- Check size, numbering, and orientation of figures.
- All images in the PDF are downsampled (reduced to lower resolution and file size) to facilitate Internet delivery. These images will appear at higher resolution and sharpness in the printed article.
- Review figure legends to ensure that they are complete.
- Check all tables. Review layout, title, and footnotes.

RETURN ☐ **CORRECTED PROOFS**
☐ **Other forms as needed**

RETURN ALL RELEVANT ITEMS WITHIN 48 HOURS OF RECEIPT

The preferred method to return corrected proofs is to return the annotated PDF to jrnlprodpen@cadmus.com.

# USING e-ANNOTATION TOOLS FOR ELECTRONIC PROOF CORRECTION

Required software to e-Annotate PDFs: <u>Adobe Acrobat Professional</u> or <u>Adobe Reader</u> (version 7.0 or above). (Note that this document uses screenshots from <u>Adobe Reader X</u>)
The latest version of Acrobat Reader can be downloaded for free at: <u>http://get.adobe.com/uk/reader/</u>

Once you have Acrobat Reader open on your computer, click on the Comment tab at the right of the toolbar:
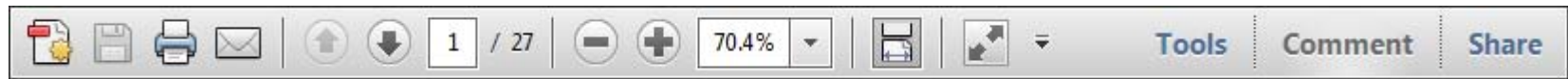
This will open up a panel down the right side of the document. The majority of tools you will use for annotating your proof will be in the Annotations section, pictured opposite. We've picked out some of these tools below:
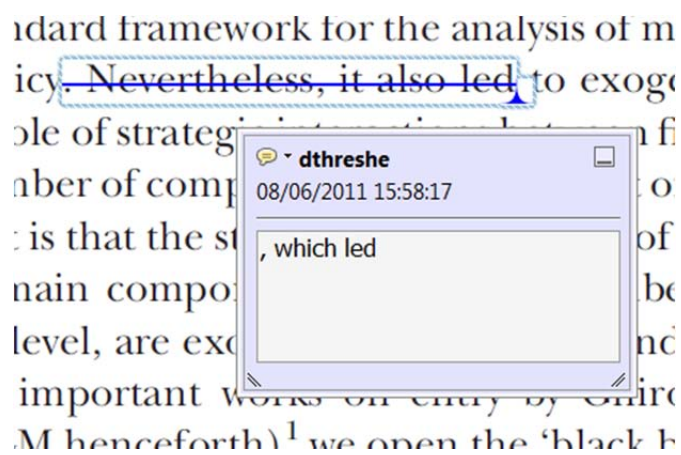
---
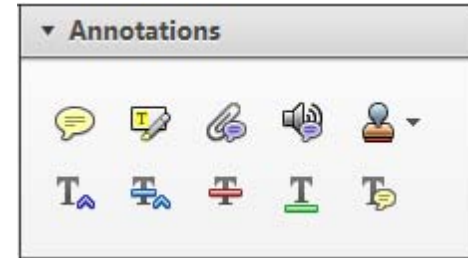
1. Replace (Ins) Tool – for replacing text.

Strikes a line through text and opens up a text box where replacement text can be entered.

How to use it

- Highlight a word or sentence.
- Click on the Replace (Ins) icon in the Annotations section.
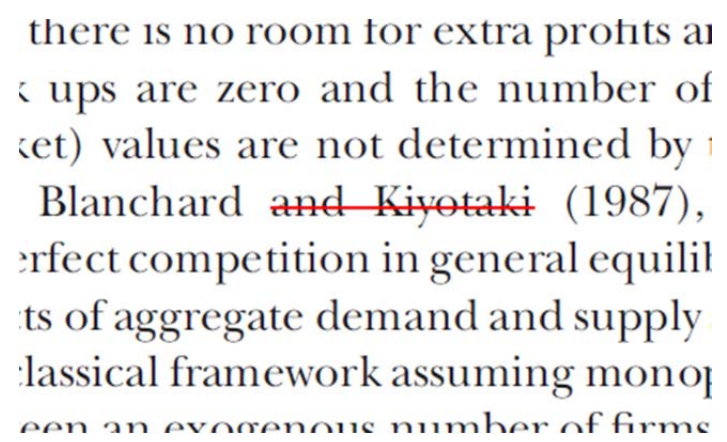- Type the replacement text into the blue box that appears.

---

2. Strikethrough (Del) Tool – for deleting text.

Strikes a red line through text that is to be deleted.

How to use it

- Highlight a word or sentence.
- Click on the Strikethrough (Del) icon in the Annotations section.

---

3. Add note to text Tool – for highlighting a section to be changed to bold or italic.
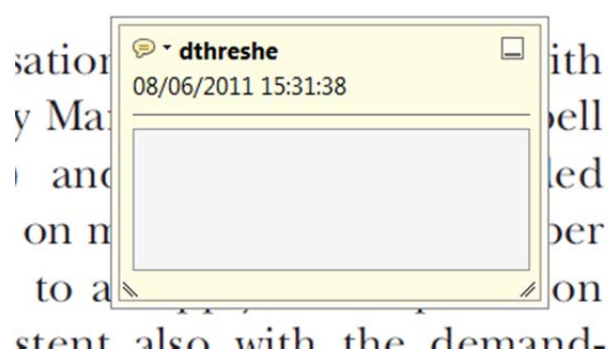
Highlights text in yellow and opens up a text box where comments can be entered.

How to use it

- Highlight the relevant section of text.
- Click on the Add note to text icon in the Annotations section.
- Type instruction on what should be changed regarding the text into the yellow box that appears.
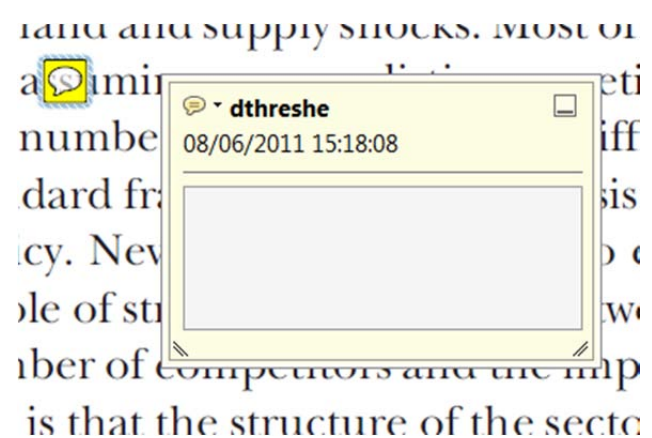
---

4. Add sticky note Tool – for making notes at specific points in the text.

Marks a point in the proof where a comment needs to be highlighted.

How to use it

- Click on the Add sticky note icon in the Annotations section.
- Click at the point in the proof where the comment should be inserted.
- Type the comment into the yellow box that appears.

# USING e-ANNOTATION TOOLS FOR ELECTRONIC PROOF CORRECTION

5. Attach File Tool – for inserting large amounts of text or replacement figures.

Inserts an icon linking to the attached file in the appropriate pace in the text.

How to use it

- Click on the Attach File icon in the Annotations section.
- Click on the proof to where you'd like the attached file to be linked.
- Select the file to be attached from your computer or network.
- Select the colour and type of icon that will appear in the proof. Click OK.

END
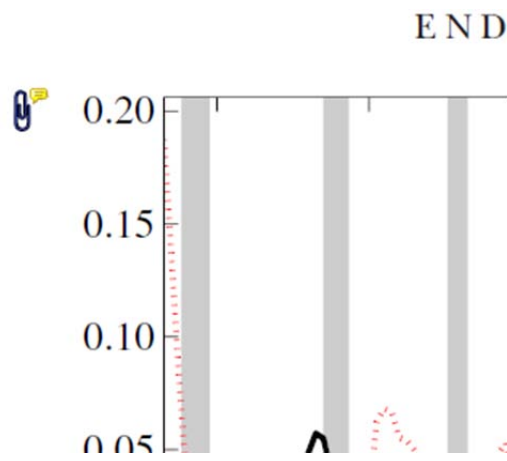
6. Add stamp Tool – for approving a proof if no corrections are required.

Inserts a selected stamp onto an appropriate place in the proof.

How to use it

- Click on the Add stamp icon in the Annotations section.
- Select the stamp you want to use. (The Approved stamp is usually available directly in the menu that appears).
- Click on the proof where you'd like the stamp to appear. (Where a proof is to be approved as it is, this would normally be on the first page).

APPROVED

Drawing Markups

7. Drawing Markups Tools – for drawing shapes, lines and freeform annotations on proofs and commenting on these marks.

Allows shapes, lines and freeform annotations to be drawn on proofs and for comment to be made on these marks..

How to use it

- Click on one of the shapes in the Drawing Markups section.
- Click on the proof at the relevant point and draw the selected shape with the cursor.
- To add a comment to the drawn shape, move the cursor over the shape until an arrowhead appears.
- Double click on the shape and type any text in the red box that appears.

dthreshe
08/06/2011 16:23:54
Move to the bottom of the left column of panels.
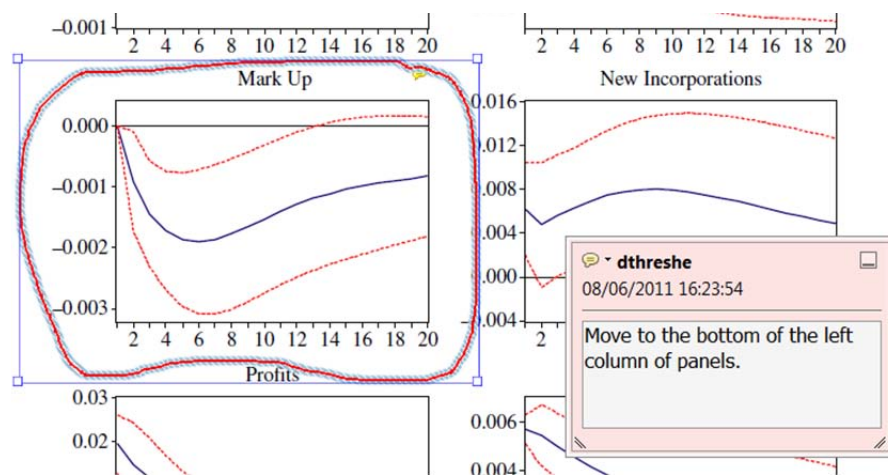
For further information on how to annotate proofs, click on the Help menu to reveal a list of further options:

WILEY-BLACKWELL
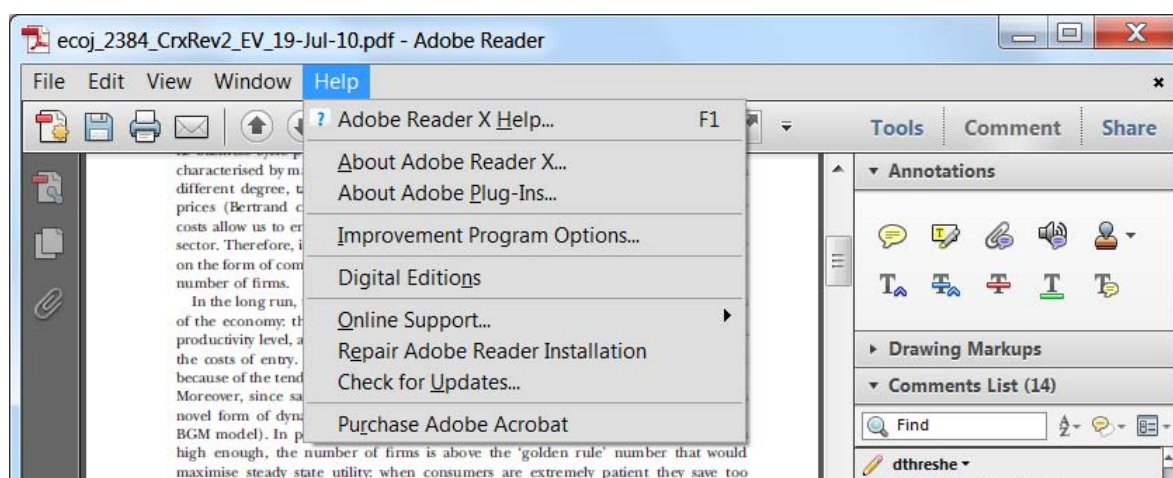
Additional reprint purchases

Should you wish to purchase additional copies of your article, please click on the link and follow the instructions provided:
https://caesar.sheridan.com/reprints/redir.php?pub=10089&acro=PEN

Corresponding authors are invited to inform their co-authors of the reprint options available.

Please note that regardless of the form in which they are acquired, reprints should not be resold, nor further disseminated in electronic form, nor deployed in part or in whole in any marketing, promotional or educational contexts without authorization from Wiley. Permissions requests should be directed to mail to: permissionsus@wiley.com

For information about 'Pay-Per-View and Article Select' click on the following link: wileyonlinelibrary.com/aboutus/ppv-articleselect.html

WILEY
Publishers Since 1807

COLOR REPRODUCTION IN YOUR ARTICLE

Color figures were included with the final manuscript files that we received for your article. Because of the high cost of color printing, we can only print figures in color if authors cover the expense.

Please indicate if you would like your figures to be printed in color or black and white. Color images will be reproduced online in *Wiley Online Library* at no charge, whether or not you opt for color printing.

Failure to return this form will result in the publication of your figures in black and white.

JOURNAL Polymer Engineering & Science   VOLUME _____   ISSUE _____

TITLE OF
MANUSCRIPT _____

MS.   NO. OF
NO. _____   COLOR PAGES _____   AUTHOR(S) _____

No. Color Pages	Color Charges	No. Color Pages	Color Charges	No. Color Pages	Color Charges
1	950	5	3400	9	5850
2	1450	6	3900	10	6350
3	1950	7	4400	11	6850
4	2450	8	4900	12	7350

Please contact the Production Editor for a quote if you have more than 12 pages of color

☐ Please print my figures in black and white

☐ Please print my figures in color $ _____

BILL TO:
Name _____

Institution _____

Address _____

_____

Purchase Order No. _____

Phone _____

Fax _____

E-mail _____

Polyethylene/Sepiolite Fibers. Influence of Drawing and Nanofiller Content on the Crystal Morphology and Mechanical Properties

Yanela Alonso,[1] Raquel E. Martini,[2] Antonio Iannoni,[3] Andrea Terenzi,[3] José M. Kenny,[3] Silvia E. Barbosa[1]

[1] *Planta Piloto de Ingeniería Química, PLAPIQUI (UNS - CONICET) Cno. La Carrindanga Km.7 - 8000 Bahía Blanca, Argentina*

[2] *IDTQ- Grupo Vinculado PLAPIQUI – CONICET, Facultad de Ciencias Exactas Físicas y Naturales, Universidad Nacional de Córdoba. Av. Vélez Sarsfield 1611, Ciudad Universitaria, 5016, Córdoba*

[3] *Civil and Environmental Engineering Department, Materials Engineering Center, University of Perugia, Località Pentima Bassa, 21, 05100 Terni, Italy*

The influence of sepiolite content (1, 2, and 3 wt%) and successive drawing steps on the final properties of polyethylene/sepiolite nanocomposite fibers are reported. Particularly the effects of these variables on crystallinity, fiber macroscopic morphology, and tensile mechanical properties are analyzed applying different experimental techniques: differential scanning calorimetry, wide angle x-ray diffraction, scanning electronic microscopy, and tensile mechanical characterization. The study evidenced the important role of both sepiolite content and stretching on the crystalline morphology and mechanical properties of the nanocomposites fiber. Both variables favor the appearance of the monoclinic phase during polyethylene crystallization, and produce an increase of crystallinity degree (35 % with drawing steps and 10 % by the sepiolite incorporation in non drawing fiber). This change of crystal morphology influences mechanical properties enhancing with both sepiolite content and drawing steps. Thus, Young Modulus ~~increase~~ 17 times with drawing in pure PE fibers and 1.5 times because sepiolite presence. The strength shows similar behavior, but the elongation at break decreases 14 timed with draw steps and to a half by the sepiolite influence. The final properties of drawing nanocomposite fibers are so acceptable for textile applications and they content particles that enhance their moisture and odors absorptive capacities. POLYM. ENG. SCI., 00:000–000, 2014. © 2014 Society of Plastics Engineers

INTRODUCTION

Polyethylene (PE) is the most used thermoplastic commodity for both industrial and consumer products, due to their good mechanical properties, chemical resistance, processability, low cost, and availability in different final forms for a wide range of applications: injected molded products, extruded tubes, and bars, films, fibers, etc. Particularly, PE fibers have great industrial interest because a considerable increase in the mechanical performance can be achieved with an appropriate mechanical stretching during fiber processing.

Pure polymers properties can be also improved through the formulation of nanocomposites taking advantage of the synergic combination of polymer and nanofiller properties. Polymer nanocomposites also allow the development of new functionalities for a certain category of products, most of them of industrial and technological interest. The main improvements that are possible to achieve with the use of nanoparticles concern mechanical performance, flame resistance, heat stability, hydrophilicity, paintability, drug release, antibacterial properties, antistatic, and UV protection, among others.

Among nanofillers, sepiolite is a low cost acicular shape clay nanoparticle with high specific surface area and excellent sorption properties, good mechanical strength and thermal stability, offering an ideal reinforcement for polymer matrices. Thus, PE - sepiolite nanocomposites are very interesting materials because they can combine the excellent mechanical properties of this polymer with the high sorption capacity of sepiolite for developing textile fibers with higher absorbency and odor neutralization [1–3]. Moreover, in the specific case of clay nanoparticles, the modification of barrier properties, water absorption and the biocide activity of the material can be also achieved [4–6].

The key factor to enhance the final properties of the nanocomposite material lies in the nanofiller-polymer intercalation and/or exfoliation. In this sense, nanoparticles with acicular morphology can be easily disaggregated because they offer less particle–particle contact area than layered clays. A family of low cost and acicular clay nanoparticles is sepiolite, which is a fibrous hydrated magnesium silicate with the theoretical half unit-cell formula $Si_{12}O_{30}Mg_8(OH, F)_4(OH_2)_4.8H_2O$. It has a structure similar to the 2 : 1 layered structure of montmorillonite, formed by two tetrahedral silica sheets enclosing a central sheet of octahedral magnesia except that the layers lack continuous octahedral sheets [7]. The discontinuous nature of the octahedral sheet allows for the formation of rectangular channels aligned in the direction of the *a*-axis, which contain some exchangeable Ca2+ and Mg2+ cations and "zeolitic water". The particular arrangement of atoms produces a needle-like structure, instead of typical plate-like one. These nanostructured tunnels account in large part for the high specific surface area and excellent sorption properties of sepiolite, which makes them extremely attractive from the industrial point of view, because it can adsorb vapor and odors and can absorb approximately its own weight of water and other liquids [8, 9]. In addition, sepiolite has good mechanical strength and thermal stability, turning this clay an ideal reinforcement for polymer materials, which has been recently used for the reinforcement of elastomers [10, 11], thermoplastic polymers [12], and biopolymers [13].

Moreover, due to their good mechanical properties, chemical resistance, processability and low cost, polyethylene (PE) is the

most used thermoplastic commodity for both industrial and consumer products. In particular, PE fibers have great industrial interest because a considerable increase in mechanical performance can be achieved with an appropriate stretching, taking advantage of the changes in the crystallization morphology induced by successive stretches, allowing their use in a wide range of applications.

In a previous work, sepiolite/PE nanocomposite films with different sepiolite concentrations were prepared by cast and their final properties analyzed. It was found that tensile and tear properties, crystallization degree, and oxygen permeability increased with the nanofiller content maintaining in all the cases, good translucency, and flexibility [14]. In the same way, and in order to develop fibers with enhanced odors, moisture, and oil absorptive properties PE/sepiolite nanocomposite fibers were formulated and processed for application in textile field mainly in carpet or special clothing. Hence, the main goal of this research is to obtain good textile fibers with the maximum amount of sepiolite, the absorptive agent. In this sense, in this work, pure PE and nanocomposite fibers were prepared varying both sepiolite content (1, 2, and 3 wt%) and successive stretching steps. The influence of these variables on the final properties of PE/sepiolite nanocomposite fibers are analyzed with particular attention to the effects on the crystallinity and tensile mechanical properties.

EXPERIMENTAL

Materials

Linear Low Density Polyethylene (PE) Dowlex 2045, kindly supplied by DOW Chemical, was used as the nanocomposite matrix. This PE has a molecular weight distribution described by M_w : 119,000 g/mol, and PD = 3.97. Sepiolite from TOLSA-Spain, was used as nanofiller. Sepiolite has acicular form and their average length is around 1.5 μm and diameter of 0.01 μm.

Compounding and Fiber Preparation

In order to enhance both, dispersion and distribution of sepiolite nanoparticles in the PE matrix nanocomposites, they were prepared in three steps by using two different twin screw extruders (TSE). Initially, masterbatches containing 10 wt% of nanofillers were compounded in a BAUSANO MD30 twin screw extruder at 40 rpm and the following temperature profile: 135–170–175°C (from feed to die). The TSE was fed with a physical mixture of PE pellets and the sepiolite previously dried under vacuum at 80°C during 24 h. In a second step, each masterbach was diluted up to final concentration in a *DSM Micro-5&15-Compounder,* and then were pelletized. This apparatus is a corotating TSE with recirculation. Three concentrations of nanocomposites, containing 1, 2, and 3 wt% of sepiolite, were prepared at 150 rpm for 1 min, with a temperature profile of 135, 160, and 190°C, from feed to die.

In the third step, fibers were obtained using a *DSM Micro-5&15-Compounder* equipped with a proper die to extrude a single filament and then it was collected by a winding unit, with a speed of J 20,000 mm/min and a torque of 75 N-mm. The temperature profile used to extrude the pellets was 135, 170, and 230°C. In order to obtain a constant diameter fiber, extrusions were performed with constant force at the head of the extruder

(300 N). Once collected the fibers on the take up roll, they have been subjected to two different single stage drawing processes in a micro fiber spin device. The stretching operation takes place between two rolls rotating at different speeds, with heating element between them. The first drawing was performed at 80°C and with a draw ratio of 2, while in the second drawing the temperature was 100°C and the draw ratio was 1.25. Both stages were performed with a rate of 100 cm/min for the roller with higher speed, while the speed of the first roller was controlled by the draw ratio input, that is the ratio between the roller speeds.

Please, note that in order to perform a complete comparison between morphological and mechanical behavior of the fibers, either pure PE or nanocomposites fibers were prepared following the same procedure, then with the same thermal and strain history.

Characterization

Diameter Measurement. r diameter of all prepared fibers was measured using a micrometer and corroborated by optical microscopy. Ten measurement of each fiber were made in different zones of the fiber.

Differential Scanning Calorimetry (DSC). lorimetric study was performed in Perkin Elmer Pyris I equipment. Thermograms were obtained directly on fiber samples heating from 25°C to 180°C and cooling from 180°C to 25°C, both at a rate of 10°C/min. Analysis was performed on the first heating cycle in order to evaluate the crystallization variation during fiber spinning and drawing steps. For this reason, the thermal history should not be removed.

Wide Angle X-Ray Diffraction (WAXS). X-ray spectra were obtained in a Philips PW 1710 diffractometer, with a graphite curve monochromator, Cu anode, 45 kv, and 30 mA. The fibers were parallel coiled on a cover glass and then were placed in the equipment. Two kinds of spectra were acquired placing the sample holder, and then the main fiber direction, parallel or perpendicular to the *x*-ray beam direction. Five spectra for each sample in each direction were performed to verify the repeatability of the technique applied.

Scanning Electron Microscopy (SEM). Morphological fiber surface analysis was carried out using a JEOL JSM-35 CF microscope equipped with secondary electron detection. The samples were coated with Au in a sputter coater PELCO 91000.

Tensile Properties ber mechanical properties were studied in an INSTRON universal dynamometer equipped with a 50 N load-cell. Ten specimens of each sample were tested at room temperature and 50 mm/min of cross head velocity on specimen of 50 mm of length.

RESULTS AND DISCUSSIONS

In a previous work [14], the distribution and dispersion of these same nanocomposites during extrusion was studied by TEM microscopy, after the second extrusion step. It was demonstrated that the filler distributes and disperses very well, but some agglomeration was detected for nanocomposites with high
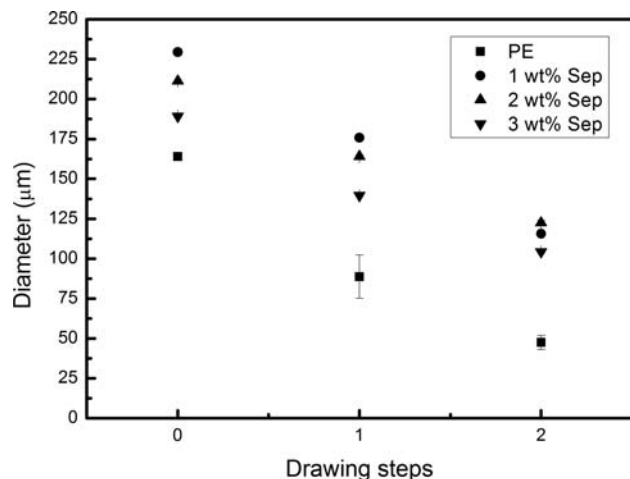
FIG. 1.   Nanocomposite fiber diameter as a function of number of drawing step for different sepiolite contents.

sepiolite content (higher than 5 wt%). This fact is not a problem for fiber spinning shown in this work because of the maximum sepiolite amount used is 3 wt%, and not agglomeration is expected during this process. Additionally, in that work a clear orientation of nanoparticles in the flow direction was demonstrated in micrographs.

F1   In Fig. 1, the results of the fiber diameter as a function of the number of drawing steps for different nanofiller content are reported. As expected, a decrease in fiber diameter with successive drawing steps is observed. The initial PE fiber diameter is lower than the nanocomposite fibers and is reduced by 70% after the second stretching, while the reduction for the nanocomposites fibers is around 50% for all concentrations prepared due to impediment in chain alignment. The lower diameter of PE fibers without drawing respect to nanocomposite ones can be explained in terms of viscosity. Fibers are pulled after die end, all with the same force. As PE has lower viscosity than composites, PE fibers stretch more than composites ones resulting in less final diameter.

On the other hand, the diameter of nanocomposite fibers decreases with the sepiolite content increase, as a consequence of the sepiolite influence in the alignment of polymer chains during fiber extrusion and drawing steps, as will be demonstrated below. However, the diameter for nanocomposite fiber with 2 wt% of sepiolite and two drawing steps is higher than the diameter of fiber with 1 wt% of nanofiller and the same drawing step. This can be due to the lower diameter reduction with drawing steps as the sepiolite amount increases.

F2   The fiber crystallinity was initially studied by DSC. In Fig. 2 the thermograms of fibers prepared with 1 wt% of sepiolite are shown. It is possible to observe that the peak height, and then the area, increases as the drawing degree increases. Taking into account that PE fibers were processed with the same thermal cycle, this difference indicates an increase of the fiber crystallinity degree induced by the polymer chain orientation during drawing. The same behavior was found for pure PE and all nanocomposite fibers analyzed. On the other hand, the thermograms for nanocomposites fusion with different sepiolite content show no evident changes, evidencing that this technique is not appropriated to discriminate the nanofiller concentration effects on crystallinity.

To elucidate the effects of both drawing steps and nanofiller content on polymer crystallization, a systematic WAXS analysis was performed by comparing spectra taken with fiber axis parallel and perpendicular to the X-ray beam. Usually, the fiber axis is close to the chain orientation direction in a fiber (meridional direction). Fibers are usually rotationally symmetric. In other words, if fibers were mounted vertically, the same diffraction pattern would be observed regardless of the φ setting. For any given 2θ range, a single sample position is required to obtain orientation information in an equatorial plane. The meridional reflections usually have a maximum intensity at the Bragg angle. This means that for an arbitrary sample position with respect to the incident beam, different crystallinity contents would be determined based on the amount of the meridional reflection in the scan. So, to determine the crystallinity, all reflections that are not on the equator must be scanned. For this reason, this study was carried out in two ways, analyzing the samples with the main direction parallel and perpendicular to the X-ray beam, matching with meridional and equatorial fiber draw direction respectively.

Polyethylene mainly crystallizes in orthorhombic structure and, in less amount, in the monoclinic one [15, 16]. In Fig. 3a,   F3
WAXS diffraction patterns of PE fibers with different drawing stages analyzed perpendicular to beam, are shown. The WAXS pattern of PE fiber without drawing is characterized by three strong peaks corresponding to the (110), (200), and (020) planes of the orthorhombic phase. These peaks are individually located at 2θ values of $21.3°$, $23.5°$, and $36.5°$, respectively. Also a very small peak occurs at about $30°$, characteristic of the monoclinic phase. As the fibers are stretched, a crystalline orientation is evidenced by the increment of the characteristic peaks, mainly the correspondent to the 110 plane. Also two little peaks typical of the monoclinic phase, appear at $13.8°$ and $16.7°$ and they increase with the drawing stage. These peaks can be assumed to correspond to the development of the monoclinic crystalline phase from the orthorhombic one, as it was demonstrated by Porter et al. [17] for PE fiber cold draw. The typical shoulder of the amorphous phase [18] around the 110 peak disappears with the drawing, confirming the increment of crystallinity degree. Moreover, there is a shifting of the peaks at $21.3°$ and $23.5°$,
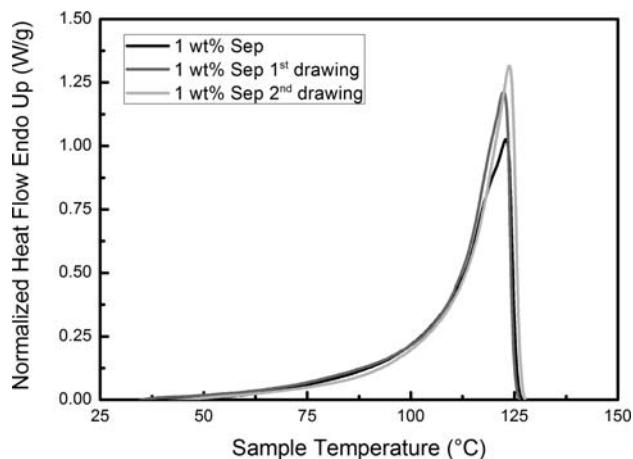

FIG. 2.   Thermograms of nanocomposite fibers prepared with 1 wt% of sepiolite at different drawing.
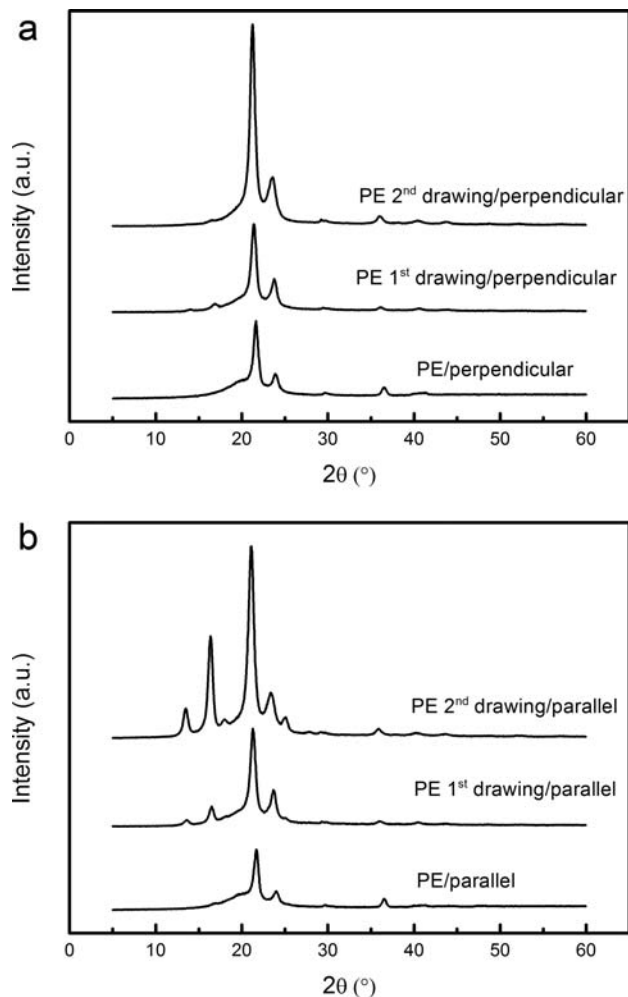
FIG. 3. Wide-angle X-ray diffraction patterns of PE fibers with different drawing stages. (a) perpendicular to the beam (b) parallel to the beam.

consistent with the variation of the crystal thickness with the drawing [19].

Several authors [20–23] have been demonstrated that monoclinic phase is usually found in polyethylene after subsequent tensile or compression deformations. This crystalline phase was found in high modulus fibers [22, 24], and it showed higher orientation than orthorhombic one [24] contributing to the improvement of its mechanical properties. In this sense, Khar'-kova et al. [22] has been concluded high crystallinity and the presence of the monoclinic modification are the necessary conditions for preparation of high modulus fibers.

The patterns obtained from the parallel analysis of the same PE fibers are shown in Fig. 3b. From this figure, it is possible to observe a higher intensity of the monoclinic phase peaks at 13.8° and 16.7° compared with the perpendicular analysis, mainly at the higher drawing stage. Not differences are detected for patterns of PE fibers obtained without drawing. Also, for PE fiber with two drawing stages two new peaks are detected at 18° and 25°, which can be attributed to the induced crystallization direction. These differences demonstrated the preferential crystal development during fiber drawing.

In the same way, the effect of sepiolite on PE crystallization was analyzed. The patterns of nanocomposites prepared with 1
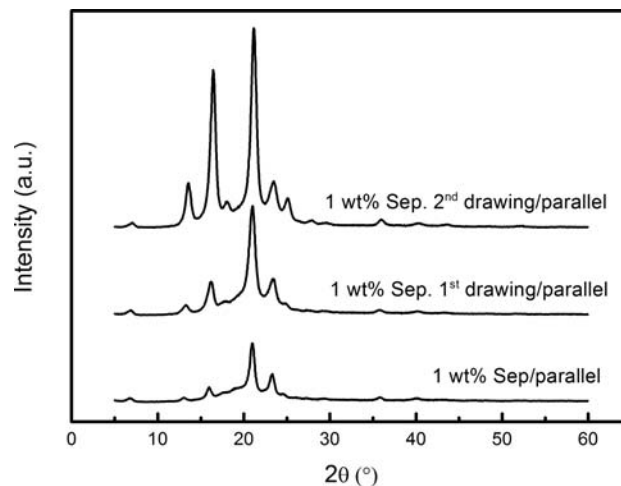

FIG. 4. Wide-angle X-ray diffraction patterns obtained parallel to the beam of nanocomposite fibers with 1 wt% of sepiolite with different drawing stages.

wt% of sepiolite obtained parallel to the beam are shown in Fig. 4. It can be seen that the presence of sepiolite evidenced by the peak at 7.1°, favors the appearance of the monoclinic phase during crystallization of PE. Unlike pure PE fibers, peaks at 13.8° and 16.7° can be observed in nanocomposite fibers without drawing. This behavior was found in both WAXS directions spectra and for all nanocomposite fibers. Also an increase of the peak height with drawing steps is detected in agreement with the previous discussion on DSC results.

The development of the monoclinic phase by the presence of sepiolite seems to depend on the sepiolite concentration. In fact, as it can be observed in Fig. 5, the typical monoclinic peak at 7.1° increases with the sepiolite concentration. Furthermore, it is observed a decrease of the peak at 36° with the sepiolite concentration. This peak corresponds to the (020) plane of the orthorhombic phase.

It is important to note that the main crystal morphology development is similar either for PE fibers with drawing increase or nanocomposite fibers without drawing as sepiolite concentration increases, mainly in the appearance and
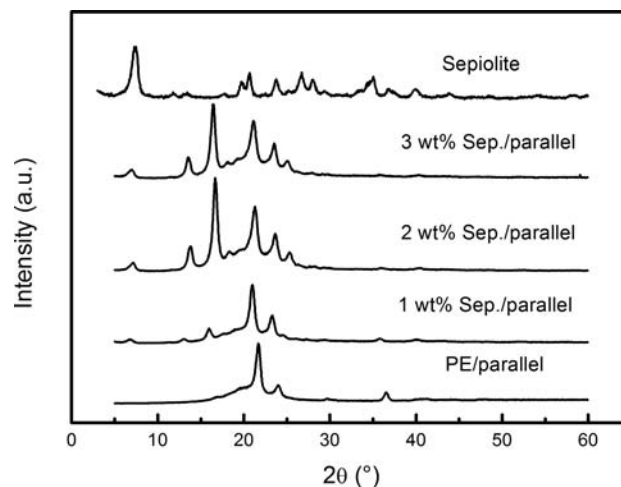

FIG. 5. Wide-angle X-ray diffraction patterns obtained parallel ~~and perpendicular~~ to the beam of nanocomposite fibers without drawing prepared with different sepiolite concentrations.
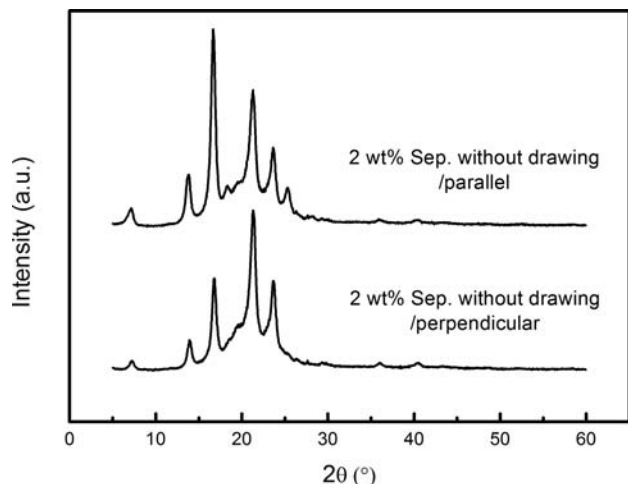
FIG. 6. Wide-angle X-ray diffraction patterns obtained parallel and perpendicular to the beam of nanocomposite fibers with 2 wt% of sepiolite without drawing.

TABLE 1. Crystallinity degree (%) of nanocomposite fibers from WAXS.

	Crystallinity (%)		
	w/o drawing	After 1st drawing	After 2nd drawing
PE	35.1	37.5	47.6
1 wt% Sepiolite	38.9	40.7	53.2
2 wt% Sepiolite	38.3	39.5	44.5
3 wt% Sepiolite	36.3	37.1	42.2

oped during drawing of linear polyethylene. The tie molecules separate of needle crystals due to the stretching tension during fiber processing and recrystallize as typical chain folded over acicular crystals, resulting in a structure similar to shish-kebab. In nanocomposites, nanofibers would "supply" the acicular geometry producing similar crystal morphology, as it is evident in Fig. 3b when compared with Fig. 5.

In Fig. 6, a comparison of WAXS patterns obtained parallel and perpendicular to the beam, of nanocomposite fibers with 2 wt% of sepiolite without drawing are presented. The intensity of the monoclinic peaks in the parallel spectrum is higher than in the perpendicular one, evidencing a preferential crystallization effect during the drawing. Otherwise, the expected sepiolite orientation in the fiber axis direction was corroborated by the

F6

growth of the peaks at $13.5°$ and $16.7°$. This behavior can be interpreted in terms of the structural model developed by Keller et al. in 1977 [25]. They proposed that acicular crystals (needle-like), aligned, and surrounded by amorphous phase, are devel-
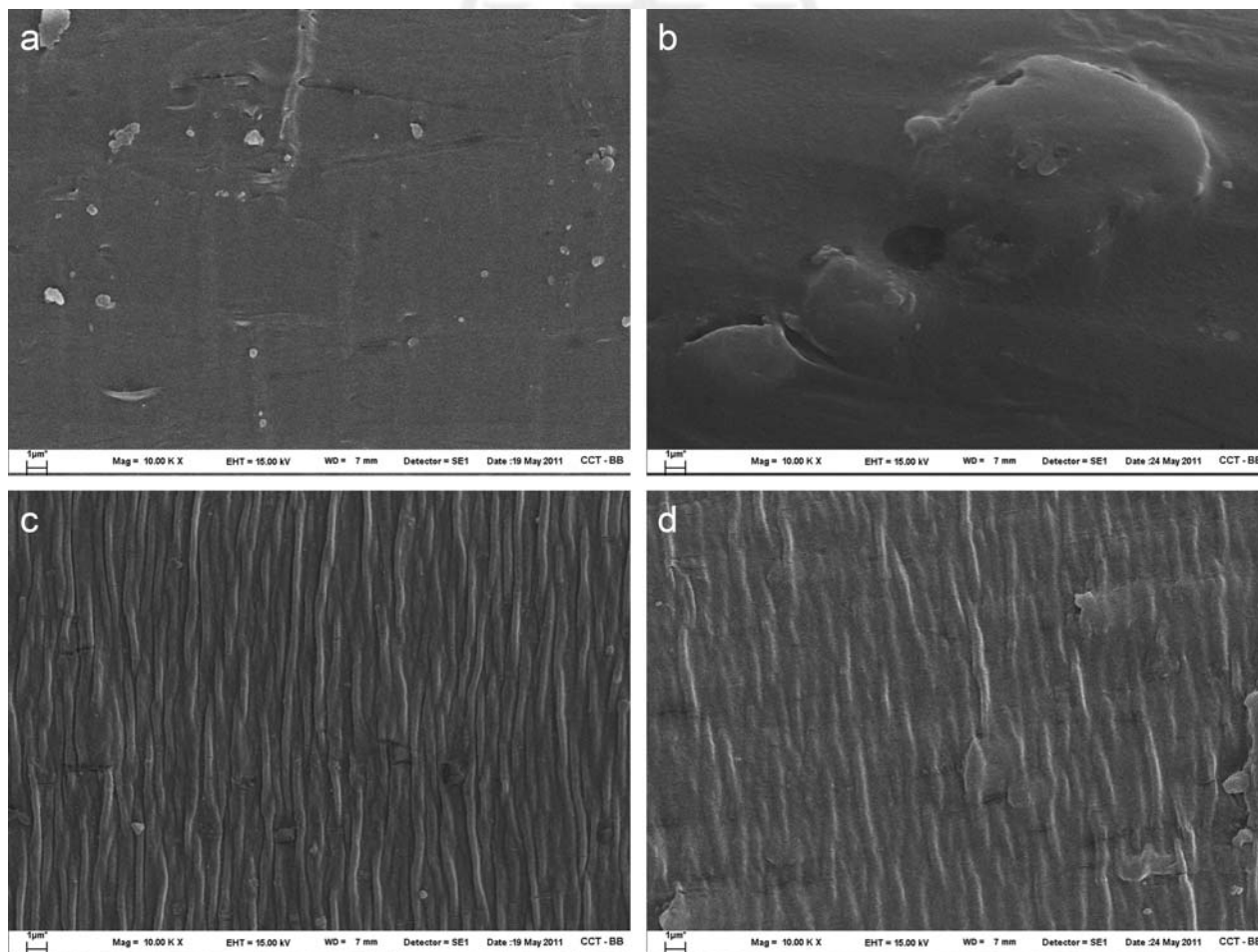

FIG. 7. SEM micrographs of a fiber after 1 drawing stage ($\times$10,000). (a) pure PE; (b) nanocomposite fiber with 1 wt% of Sepiolite; (c) nanocomposite fiber with 2 wt% of Sepiolite; (d) nanocomposite fiber with 3 wt% of sepiolite.
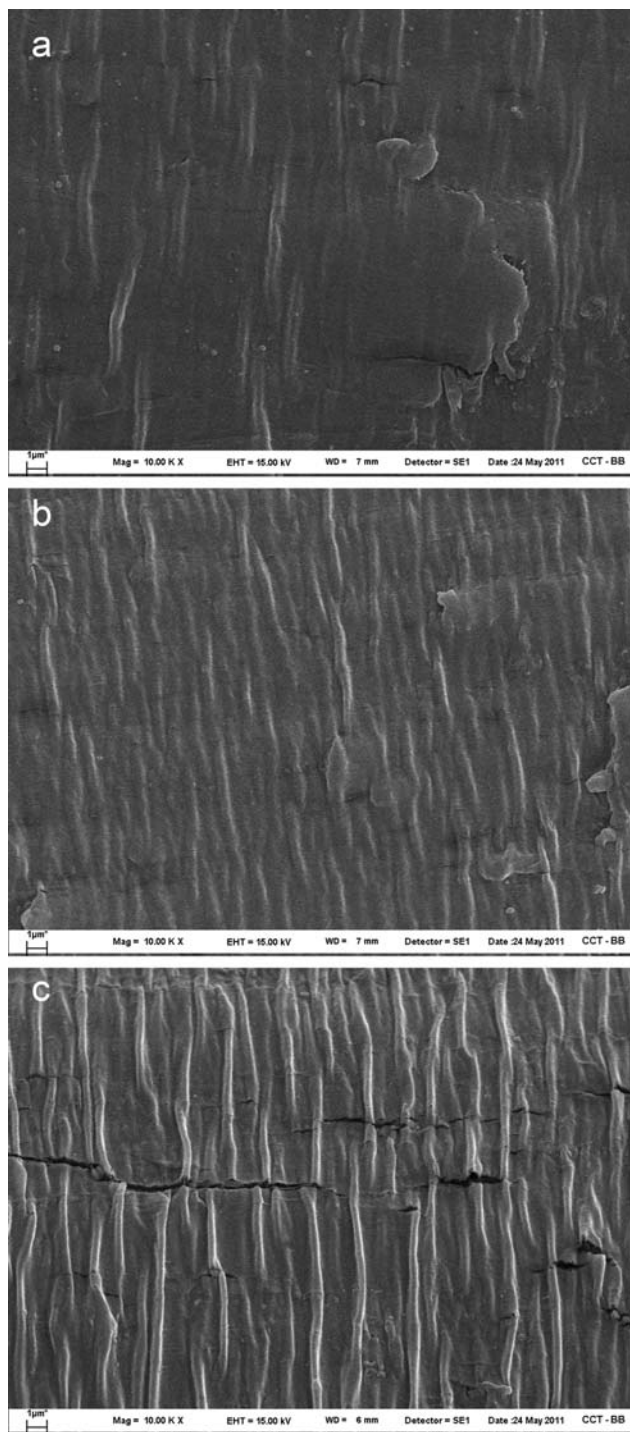
FIG. 8. SEM micrographs of a fiber with 3 wt% of sepiolite (×10,000). (a) Without drawing. (b) After one drawing stage; (c) After two drawing stages.

higher intensity of its typical peak (7.1°) in samples analyzed parallel to the beam than in the perpendicular one.

The crystallinity degrees of each sample calculated from the WAXS spectra are listed in Table 1. The nucleating effects of sepiolite can be confirmed by the increase of crystallinity with the nanofiller content. Also, the effect of drawing on fiber crystallinity can be noticed, resulting in an increase in crystallinity

up to 60% after the second drawing. However, it can also be observed that the increasing crystallinity produced by drawing in the fibers of pure PE and in the nanocomposite with 1 wt% of sepiolite is higher than in the nanocomposite fiber prepared with 2 and 3 wt% of nanofiller. These results agree with the observation made on the fiber diameter, thus confirming that the presence of sepiolite hinders PE chain alignment either during fiber extrusion or drawing operations. The maximum crystallinity increment by nanofiller presence is about 10%, showing a lower effect on this property than the drawing step.

Fiber surface morphology was studied in order to detect macroscopic defects. In Fig. 7 SEM micrographs of the surface of both PE and nanocomposite fibers prepared after the first drawing stage, are shown. A smooth surface with a small presence of particles of the same polymer is observed both for PE and for the nanocomposite with 1 wt% sepiolite. However, as the filler content increases, fibers present a rough surface with entire bands and rows of etched pockets in the transversal direction with respect to the fiber axis. This kind of superficial defect, called "Pisa Structure," was detected by other authors in pure PE and nanocomposite fibers during drawing [26–28]. They attributed this kind of defects to the mobility and then with a drawability of the polymer chains. This result agrees with the smaller diameter reduction and smaller crystallinity increment with stretching steps found in nanocomposite fibers with respect to the PE ones. The two last aspects are strongly related with the lower drawability observed in nanocomposite fibers as a consequence of a lower chain mobility due to the nanofiller presence. In the same way, the defects appear to increase with successive drawing stages, as it can be observed for fibers with 3 wt% of sepiolite in Fig. 8, in concordance with a lower capability of the polymer chains to be extended in successive stretching steps.

The polymer chain alignment with successive drawing stages and the associated crystallinity increase have a direct effect on fiber mechanical properties. In Table 2 the main mechanical properties of fiber prepared are listed. The reinforcement effect of sepiolite is confirmed by the modulus increment with sepiolite content in fibers without stretching and with 1 drawing stage. Moreover, the modulus obtained for fibers with two

TABLE ●●

Young Modulus (MPa)			
	w/o drawing	1 drawing	2 drawing
PE	113.56 ± 21.44	215.33 ± 25.32	1919.97 ± 530
1 wt% Sepiolite	135.92 ± 53.21	192.29 ± 16.15	1388.76 ± 638.68
2 wt% Sepiolite	129.90 ± 75.84	216.54 ± 75.60	1087.19 ± 490.22
3 wt% Sepiolite	167.87 ± 82.61	250.98 ± 51.28	1117.70 ± 252.39
Elongation at peak (%)			
PE	791.99 ± 239.94	169.63 ± 147.26	55.71 ± 20.30
1 wt% Sepiolite	658.00 ± 108.65	199.58 ± 57.81	50.67 ± 17.08
2 wt% Sepiolite	466.98 ± 250.84	266.93 ± 99.81	69.15 ± 27.18
3 wt% Sepiolite	346.38 ± 198.96	203.47 ± 45.48	58.42 ± 12.98
Yield Strenght (MPa)			
	w/o drawing	1 drawing	2 drawing
PE	20 ± 3	76 ± 7	538 ± 12
1 wt% Sepiolite	25 ± 2	65 ± 5	305 ± 23
2 wt% Sepiolite	48 ± 4	55 ± 5	246 ± 15
3 wt% Sepiolite	55 ± 4	62 ± 4	239 ± 13

drawing stages strongly increase by several orders of magnitude. This relevant increment is higher than the corresponding crystallinity increase due to the drawing, showing that the change in crystal morphology is the main factor affecting the mechanical properties improvement. Moreover, for the second drawing an opposite trend is observed when the sepiolite content increases. In this case, a decrease in modulus values as nanofiller content increases is observed. This confirms the higher hindrance introduced by the presence of nanofillers on the alignment of the polymer molecules and this agrees with the observations of Keller [25] and the justification presented in the model as a function of the crystal morphology previously explained. The increment on polymer rigidity with drawing is also reflected in the decrease in strain at break. From Table 2, it can be also observed a decrease in elongation at break as the sepiolite content increases, in agreement with more defects found by SEM in nanocomposite fiber with higher sepiolite content.

In the same way, strength is increased with both drawing stages and sepiolite content, as it can be observed in Table 2. From these data, it can be claimed that the drawing stage is more effective than the clay content for mechanical properties improvement. Moreover, a saturation of the reinforcement effect is observed with 2 wt% of sepiolite, in fact not relevant differences are observed in comparison with 3wt% nanocomposite. Similar behavior was observed in films prepared with the same nanocomposite material [14]. Alike the Young Modulus, the strength increment by stretching is higher for PE than for the nanocomposites fibers, and then the strength for PE with two drawing stages is slightly higher for the nanocomposite fibers with the same stretching degree.

CONCLUSIONS

In this work, the influence of both sepiolite content (1, 2, and 3 wt%) and successive drawing steps on the final properties of PE/sepiolite nanocomposite fibers has been studied in order to analyze their use in textile field. In this sense, the effects of nanoparticles concentration and successive drawings on fiber macroscopic morphology, crystallinity, and tensile mechanical properties have been analyzed.

The initial PE fiber diameter is lower than the nanocomposite fibers ones and is reduced by 70% after the second stretching, while the reduction for the nanocomposites fibers is around 50%. The difference in diameter reduction was explained in terms of different phenomena that governed stretch behavior of each fiber as explained above.

PE fibers has a smooth surface, but some particular defects are evidenced in nanocomposite ones. These defects, named "Pisa structure" proceeds from the lower drawability of nanocomposite fibers and do not notably reduce the mechanical properties of this kind of fibers as showed above, because they are mainly influenced by crystallinity morphology variation. These defects increase with drawing steps.

Regarding crystallinity analysis, both variables, sepiolite content, and successive drawing steps, favor the appearance of the monoclinic phase during polyethylene crystallization, and produce an increase of crystallinity degree (35% with drawing steps and 10% by the sepiolite incorporation in non drawing fiber).

For this reason the crystallinity changes in drawn nanocomposite fibers is lower than drawn pure PE fibers. The change of crystal morphology influences mechanical properties enhancing also with both sepiolite content and drawing steps, being higher the effect of the drawing stages due to the predominant effect of the chain alignment on these properties. Thus, Young Modulus increase 17 times with drawing in pure PE fibers and 1.5 times because sepiolite presence. The strength shows similar behavior, but the elongation at break decreases 14 timed with draw steps and to a half by the sepiolite influence.

Sepiolite/PE nanocomposite fibers result a very interesting material to be used in textile industry, because they conserve good mechanical properties with high fiber concentrations and drawings and have the possibility to be absorbed moisture, being so important material for carpet fabrication.

REFERENCES

1. M. Shafiq,T. Yasin, and S. Saeed, *J. Appl. Polym. Sci.*, **123**, 1718 (2012).

2. N. García, M. Hoyos, J. Guzmán, and P. Tiemblo, *Polym. Degrad. Stabil.*, **94**, 39 (2009).

3. M. Arroyo, F. Perez, and J.P. Vigo, *J. Appl. Polym. Sci.*, **32**, 5105 (1986).

4. R. Magaraphan, W. Lilayuthalert, A. Sirivat, and J.W. Schwank, *Compos. Sci. Technol.*, **61**, 1253 (2001).

5. A. Durmuş, M. Woo, A. Kaşgöz, C.W. Macosko, and M. Tsapatsis, *Eur. Polym. J.*, **43**, 3737 (2007).

6. R. Nigmatullin, F. Gao, and V. Konovalova, *J. Mater. Sci.*, **43**, 5728 (2008).

7. S. Xie, S. Zhang, F. Wang, M. Yang, R. Séguéla, and J.-M. Lefebvre, *Compos. Sci. Technol.*, **67**, 2334 (2007).

8. F. Caturla, M. Molina-Sabio, and F. Rodriguez-Reinoso, *Appl. Clay Sci.*, **15**, 367 (1999).

9. E. Galan, *Clay Minerals*, **31**, 443 (1996).

10. L. Bokobza, A. Burr, G. Garnaud, M. Perrin, and S. Pagnotta, *Polym. Int.*, **53**, 1060 (2004).

11. L. Bokobza, *J. Appl. Polym. Sci.*, **93**, 2095 (2004).

12. J.Z. Rong, X. Hong, and W. Zhang, *Polyolefin-Clay Nanocomposites and Process for the Preparation Thereof*. 2002.

13. M. Darder, M. Lopez-Blanco, P. Aranda, A.J. Aznar, J. Bravo, and E. Ruiz-Hitzky, *Chem. Mater.*, **18**, 9 (2006).

14. R.E. Martini, S. La Tegola, A. Terenzi, J.M. Kenny and S.E. Barbosa, *Polym. Eng. Sci.*, n/a (2013).

15. D. Olmos, C. Domínguez, P.D. Castrillo, and J. Gonzalez-Benito, *Polymer*, **50**, 1732 (2009).

16. Q. Yuan, R. Gudavalli, and R.D.K. Misra, *Mater. Sci. Eng. A*, **492**, 434 (2008).

17. W.T. Mead, C.R. Desper, and R.S. Porter, *J. Polym. Sci. Polym. Phys. Ed.*, **17**, 859 (1979).

18. Z.W. Wilchinsky, *J. Polym. Sci. Part A-2: Polym. Phys.*, **6**, 281 (1968).

19. J. Clements and I.M. Ward, *Polymer*, **24**, 27 (1983).

20. R. Popli and L. Mandelkern, *J. Polym. Sci. Part B: Polym. Phys.*, **25**, 441 (1987).

21. N.S.J.A. Gerrits and R.J. Young, *J. Polym. Sci. Part B: Polym. Phys.*, **29**, 825 (1991).

AQ1

22. E.M. Khar'kova, D.I. Mendeleev, V.A. Aulov, B.F. Shklyaruk, V.A. Gerasin, A.A. Piryazev and A.E. Antipov, *Polym. Sci. Series A*, **56**, 72 (2014).

23. C.R. Desper, (1989).

24. I. Karacan, *Fibres Text. Eastern Eur.*, **13**, 15 (2005).

25. R.G.C. Arridge, P.J. Barham, and A. Keller, *J. Polym. Sci. Polym. Phys. Ed.*, **15**, 389 (1977).

26. T. Amornsakchai, R.H. Olley, D.C. Bassett, M.O.M. Al-Hussein, A.P. Unwin, and I.M. Ward, *Polymer*, **41**, 8291 (2000).

27. T. Amornsakchai and P. Songtipya, *Polymer*, **43**, 4231 (2002).

28. S. Chantrasakul and T. Amornsakchai, *Polym. Eng. Sci.*, **47**, 943 (2007).

AQ1: Please provide complete details for Refs. 12, 14, 23.

AQ2: Please provide the caption for Table 2